Irrigation Sciences and Engineering (JISE) Vol. 43, No. 4, Winter 2021, Original Paper p. 63-78

The effect of fluctuations in moisture on resistance to soil erosion in the process of dust production (Case study of Lake Bazangan , Iran)

Mahya Hassanzadeh Eskafi[1], Kazem Esmaili[2*] and Saeed Reza Khodashenas[3]

1- Master Student, Department of Water Science and Engineering, Faculty of Agriculture, Ferdowsi University of Mashhad.
2*- Corresponding Author, Associate Professor, Department of Water Science and Engineering, Faculty of Agriculture, Ferdowsi University of Mashhad.*(esmaili@um.ac.ir).*
3- Professor, Department of Water Science and Engineering, Faculty of Agriculture, Ferdowsi University of Mashhad.

Received: 26 December 2020 Revised: 21 February 2021 Accepted: 24 February 2021

Abstract

The drying of lakes and wetlands is a significant challenge to the hydrological cycle of resources, to human life, and to animal and plant species. The bed soils of lakes in arid and semi-arid regions become dry and wet due to various factors, such as global warming, which decrease and increase water levels in lakes. Therefore, field measurements and surveys are necessary in the localities of these natural ecosystems and can improve the management and protective measures against various hazardous processes including wind-driven soil erosion in these areas. The purpose of this research was to evaluate the soil erosion potential of Lake Bazangan, a natural lake located in the province of Khorasan Razavi, Iran. Experiments of soil properties were performed to study the rate of soil wind erosion. Wind tunnels were used to model the airflow. The results showed that the clay particle content significantly reduced soil wind erosion rates. Because of SAR's effect on the dispersion of clay particles, the erosion rate increased exponentially with soil solidification. Soil moisture had a significant effect on the cohesion of clay particles and, therefore, reduced the soil wind erosion rate. In this study, the surface erosion of the samples was examined using a calibrated Kinect® sensor, developed by Microsoft, due to easy access, cost-effectiveness, and high accuracy of its sensors. It was observed that sand particles could move easily, with a significant effect on the rate of soil loss.

Keywords: Particle distribution; Wet and dry; Shear strength; Wind tunnel; Laser scanning.
DOI: 10.22055/jise.2021.36299.1948.

Introduction

Human life continues from water, soil, and air elements. In recent years, natural habitats in different parts of the world have been destructed by humans and by various factors in which they have played a key role. Environmental endangerment has been a serious threat to future generations of plant and animal species. Global warming is one of the most important threatening factors. In arid and semi-arid regions, the hydrological cycle of river basins and water resources is strongly influenced by climate change (Afshar et al., 2017). Rising greenhouse gases and climate change lead to changes in natural ecosystems. One such change is the drying of lakes and wetlands. With the drying of lakes, the bed soils of the lakes dry in the course of time and can move if exposed to different wind fronts. Dust can originate from upstream areas or be transported locally from the ground surface (Roney and White, 2006), leading to environmental pollution in the surrounding areas. Climate change and population growth

increase the harvest of surface and groundwater sources, which can dramatically raise possible drying of these water sources.

Many extensive sources of dust are affected by shallow groundwater as shallow groundwater can contribute to dust production and, in severe cases, may lead to desertification in semi-arid regions (Elmore et al., 2008). Wind erosion annually generates 500-5,000 tons of dust (Grini et al., 2005). The main factors influencing dust storm activity are wind speed and direction, drought, and high temperatures, which affect the soil strength coefficient by vegetation, soil texture, and soil structure (Orlovsky et al., 2005). Damages to agriculture from wind erosion include sedimentation, soil degradation, and crop loss (Sterk, 2003). Airborne dust may involve in a variety of reactions and form new compounds in the atmosphere (Gile and Grossman, 1979). Studies on the impact of dust from wind erosion on climate quality and environmental conditions have revealed that carbonate-containing dust may cause acid rain in areas without nitrogen oxides and sulfur (Zhang et al., 2003). Soil surface moisture is the most important factor affecting wind erosion and sediment transport by the wind so that elevated soil surface moisture reduces soil erosion and controls the rate of erosion to a high extent (Pye, 1994). Also, soil moisture plays a significant role in erosion (Singh and Thompson, 2016). In Mongolia, research on the relationship between soil moisture and dust emission in a sandy soil layer demonstrated a great impact of soil moisture on the limit velocity of soil particles and dust reduction rate (Munkhtsetseg et al., 2016). Prolonged wind erosion was reported to result in soil dryness and sand accumulation, reducing soil water content (Zhao et al., 2006). In Lake Owens, southeastern California, which was dried up in 1924 due to the construction of the Los Angeles Aqueduct for rainwater accumulation in the Owens River, particles were dispersed into the air from the surface of the dry bed of the lake in spring and autumn with severe dust storms (Kim et al., 2000).

Physical and chemical properties of soil play a pivotal role in soil erosion by wind (Gillies et al., 2017).

Soil properties such as soil texture, shear strength and soil particle size affect the wind speed of the particle movement threshold, which is the minimum speed required to start moving (Goossens, 2004) and (Shao, 2008). The most influential chemical properties of soil that affect soil erodibility are the electrical conductivity (EC) of soil and its sodium absorption ratio (SAR) (Panayiotopoulos et al., 2004). One of the important factors for studying soil stability and structure in semi-arid regions is SAR (Emami et al., 2014). Increasing the concentration of dissolved sodium increases SAR and soil sensitivity to wind erosion (Zobeck et al., 2013).

Wetlands are important ecosystems for biodiversity conservation (Biglarfadafan et al., 2016) and play an important role in the hydrological cycle of resources and river droughts (Maltby and Acreman, 2011). Waterfowl were also found to prefer natural lakes and wetlands to man-made lakes (Behrouzi-Rad, n.d.). According to the above-mentioned studies, the drying of lakes and wetlands has many negative effects that may threaten human life as well as animal and plant species. Accordingly, it is necessary to study the conditions of wetlands and lakes to assess the potential of soil movement. Despite the fact that Lake Bazangan is the only natural lake in northeastern of Iran, which is located in Sarakhs and is the habitat of various plant species, there are several reasons leading to its destruction. Sarakhs region is exposed to strong winds and there are few studies on the prevention of the destruction of this natural habitat . Therefore, the present study can play a crucial role in order to protect this natural habitat and can contribute to controlling wind erosion in Lake Bazangan. We evaluated the potential of soil erosion by wind in the bed of Lake Bazangan. In this sense, we gathered the samples and measured the physical and chemical properties of the lake's bed, which were sunk previously and it is dry now. Soil samples were placed in a constant wind tunnel. By applying the dominant wind speed of the

 DOI: 10.22055/jise.2021.36299.1948.

area, the relationship between the erosion rate potential of the soil from the lake's bed and the physicochemical properties was studies in two different humidity conditions. Finally, Microsoft's Kinect® sensor was utilized for different samples to obtain the eroded soil profiles.

Materials and methods

Study area

Sarakhs is located in the northeast of the province of Khorasan Razavi in the northeast of Iran (Figure. 1a). This city has an arid and semi-arid climate with optimum conditions which play a role in generating dust and wind erosion (Choobari et al., 2014). Lake Bazangan is located around the city of Sarakhs in the geographical coordinates 36° 18′ 36″ to 36° 19′ 6″ N and 60° 28′ 32″ to 60° 29′ 5″ E (Figure. 1b). The lake is known as the largest natural lake in eastern Iran. Meteorological data of the study area were collected from the World Weather Online (Figure. 2). The water of Lake Bazangan is supplied by precipitation, surface water, and deepwater sources.

The bed soil wind erosion potential of Lake Bazangan has been evaluated in the present study. The meteorological data, such as wind speed, contributes to estimating wind erosion and can be used to analyze the factors affecting soil erosion (Stetler and Saxton, 1997). According to Khorasan Razavi's Meteorological Organization, winds of more than 15 m/s occur mostly in mid-January and July in the city of Sarakhs (Karimi et al., 2017).

Ziyaee et al. (Ziyaee et al., 2018) cited several studies indicating that loess deposits, which are part of the south of Mashhad (Karimi et al., 2009) and are located in Kopeh Dagh mountains (Karimi et al., 2014; Okhravi and Amini, 2001), and the sand dunes which are stabilized are evidence of strong winds in this province. In Sarakhs, the main causes of wind erosion are water level, wind speed, and shear stress (Ziyaee et al., 2018). Moist winds can cause rain in some areas, and hot dry winds can sometimes cause drought, fires, and crop losses.

According to Khorasan Razavi Environment Organization (www.rko.doe.ir), Lake Bazangan is affected by hot dry winds due to its proximity to the Qarahqom desert in Turkmenistan. As such, elevated air temperatures and decreased flow of springs and surface currents have led to dropped groundwater level of this lake. Sandstorms are caused by dry weather, strong winds, and scattered vegetation (Chen et al., 1996).

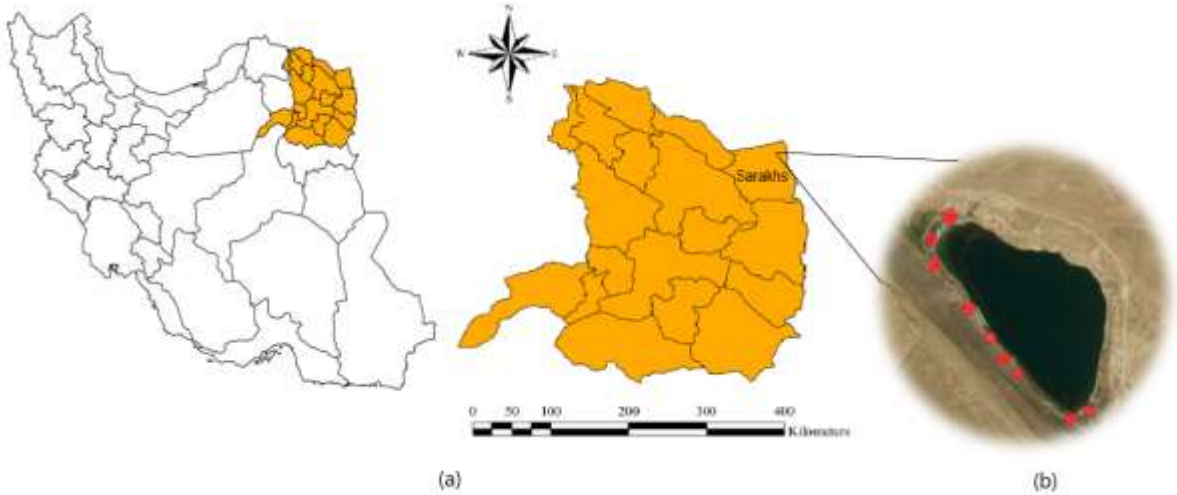

Fig.1- Different regions selected from 9 sites in Lake Bazangan, Sarakhs, Khorasan Razavi province

Soil sampling points were selected using aerial images of Lake Bazangan in different years to determine the coordinates of currently dried points around the lake and the underwent water level fluctuations in the past. The location of samples and the geographical coordinates of the sampling points are shown in Figure (1b). Holes were dug on the ground surface of sampling points by an auger, the hole volume was estimated through an equivalent volume of water, and the soil bulk density was determined by the balloon method. Collected samples were placed in a plastic bag to prevent changes in their moisture content until the tests (Figure. 3).

Wind erosion leads to the transfer of soils as well as surface soil chemicals and creates interregional dust (Van Pelt and Zobeck, 2007). The effect of soil moisture on dust emissions was investigated in the Horqin Sandy Land area during 2011-2015. The study showed that the effect of moisture was visible on a monthly time scale (Ju et al., 2018). Soil moisture cohesion is an important factor in wind erosion resistance. The amount of soil moisture that impacts soil erosion was investigated in northern China by wind tunnel. There was a negative correlation between wind erosion rate and content of moisture soil so that the initial wind erosion rate decreased relatively quickly by increasing soil moisture (Chen et al., 1996).

A set of physical and mechanical tests of soils, including granulation, soil texture, and estimation of shear strength were performed on the samples transferred to the laboratory. Granulation tests for coarse- and fine-grained particles were performed by sieving and the hydrometric method (hydrometer 152H), respectively.

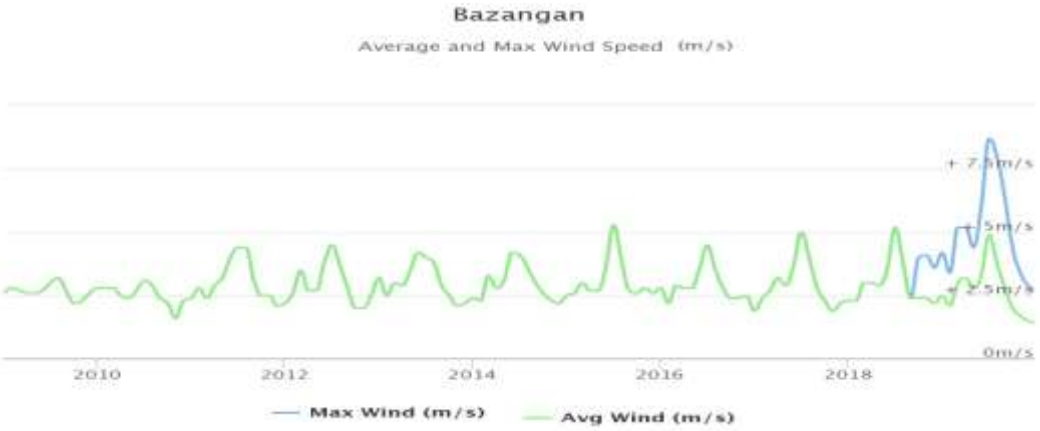

Fig.2- Average and maximum wind speeds (m/s) measured between 2010 and 2019 at Lake Bazangan

Fig. 3- General views of the study area and sampling of Lake Bazangan

 DOI: 10.22055/jise.2021.36299.1948.

In this study, in order to determine the parameters of shear strength of soil samples, particle adhesion resistance (C) and internal friction angle (φ) according to ASTM D 3080 standard, a direct cutting machine was used (Figure 4). The experiments were performed without drainage and the soils were subjected to direct shear testing at selected moisture levels. In this experiment, the shear and horizontal displacement forces to cut the sample had to be measured. Using shear stress and vertical stress values for all samples, the adhesion parameters (C) and the internal friction angle (φ) were calculated (Astm, 1994). Equation 1 (Columbus equation) was used as the basis for determining the coefficients C and φ, which were determined by performing several shear tests on each soil sample:

$$\tau_f = C + \sigma \tan\varphi \qquad (1)$$

In Equation (1), τ_f is the shear stress, σ is the vertical stress in the rupture plane, φ is the internal friction angle, and C is the adhesion between the soil particles.

Experimental conditions in terms of soil moisture and natural soil density were simulated by *in situ* determination of soil bulk density to make the results as compatible with the natural condition as possible. The chemical properties of the studied soil samples were investigated by preparing saturated mud extract of the samples. EC, pH, SAR, ESP, and the amounts of Na^+, Ca^{2+}, and Mg^{2+} were then measured to evaluate the soil salinity and the soil sodium concentration potential. Organic matter contributes to the stability and formation of soil structure (Emami et al., 2012). Many studies (Chepil, 1954) investigated the effect of organic matter on wind-driven soil erosion. The salinity level of saturated mud extract samples was measured using an EC meter. Soil and water salinity is a combination of different ion types (Ben-Gal et al., 2009). The pH of each saturated extract of soil sample was measured using a pH meter calibrated by buffer solutions. Soluble cations in each sample of saturated mud extract were measured by a flume photometer, and calcium and magnesium ions were measured by the titration method (Richards, 1954). One of the important factors for soil stability and structure in semi-arid regions is SAR (sodium adsorption ratio) analysis (Emami et al., 2014). Using the obtained concentrations of cations, SAR was determined by Equation (2).

$$\text{SAR} = \frac{Na^+}{\sqrt{\left(\frac{Mg^{++} + Ca^{++}}{2}\right)}} \qquad (2)$$

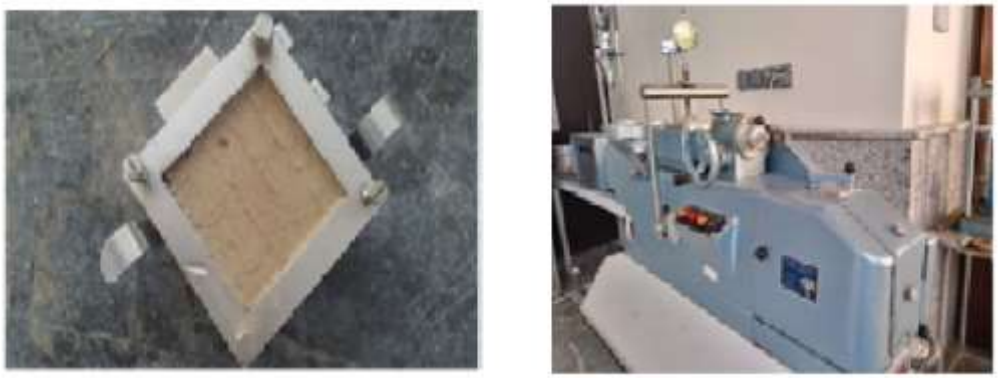

Fig. 4- Direct shear test equipment (a) direct shear (b) sample in the straight cut

Wind erosion modeling

A method for obtaining information about the production of fine particles is the physical modeling of wind erosion in a wind tunnel (Gillette, 1978). Using a wind tunnel allows the study of some influential factors such as wind speed forces, particle size, and time after deposition (Nicholson, 1993). In Spain, a study was conducted in a semi-arid region (Welsons) from 1996 to 1999 to evaluate the potential effects of land use change and land use management on soil wind erosion in agricultural land (Gomes et al., 2003). To investigate the potential of soil erosion, site samples were compacted with site density. Then, the erosion potential of soil samples was examined at different moisture levels by a wind tunnel in the laboratory of water sciences and engineering, Ferdowsi University of Mashhad (Figure 5). The wind tunnel used here was an open flow wind tunnel with the ability to simulate wind up to a speed of 30 m/s. The total length, the size of glass sampling section, and the width of the wind tunnel were 4.5 m, 0.5 m, 0.3 m, and 0.3 m, respectively. The body of this device was equipped with a speed measuring sensor of the vane anemometer type, easily measuring the wind flow speed and the incoming air temperature with a high accuracy for the user. This device consists of three main parts, namely the wind generator, the experimental section, and the sediment trapping section (Figure 6).

Since the samples must be located in an area with a developed and uniform flow, the location of samples in the glass box was determined by considering the governing boundary layer conditions, which are based on Prandtl's theory results used as a standard tool for wind tunnel data since the late 1920s (Anderson, 2005).

Fig. 5- The wind tunnel deployed in the laboratory

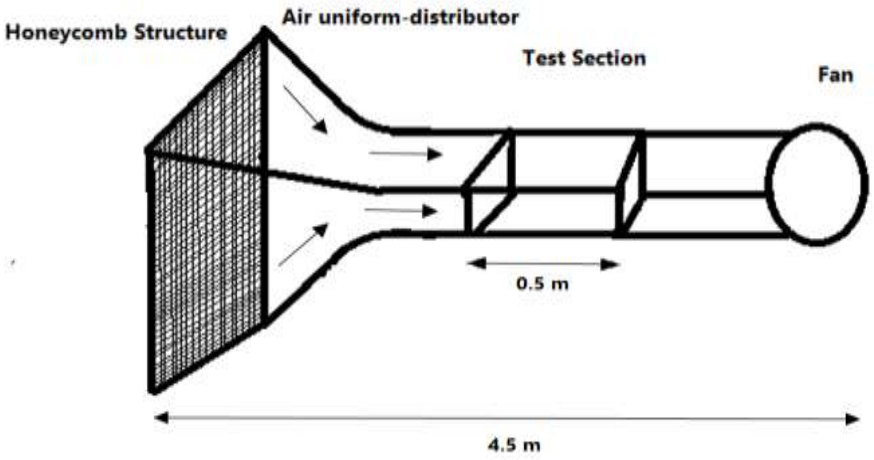

Fig. 6- Different parts of the wind tunnel used in the study

 DOI: 10.22055/jise.2021.36299.1948.

The boundary layer thickness was calculated by the following equations according to the dimensions of the sampling place, and the samples were finally placed where the flow was fully developed and uniform.

The Reynolds number was calculated according to Equation (3):

$$R_e = \frac{v \times D}{\vartheta} \quad (3)$$

where v is the air flow velocity, v is the air viscosity ($1.8 \times 10^{-5}\ \frac{m^2}{s}$) inside the wind tunnel, and D is the hydraulic diameter of the wind tunnel calculated by Equation (4):

$$D = \frac{4\,A}{P} \quad (4)$$

where A and P are the cross-sectional areas of the sampling location and the wind tunnel, respectively.

Because the flow regime was turbulent based on the calculation of the Reynolds number, the thickness of the boundary layer was determined by Equation (5), where X is the sample distance from the beginning of the wind tunnel.

$$\delta = \frac{0.37X}{(R_x)^{\frac{1}{5}}} \quad (5)$$

According to the calculations of the boundary layer thickness using the above equations, the samples were placed in a location with a distance of at least 7 mm from transverse, lower, and upper walls around the wind tunnel so that the samples were protected from the effects of air flow.

Sampling location and wind flow duration were considered the same for all soil samples to investigate the relationship between erodibility soil and soil properties during the wind speed test. Each soil sample was placed inside the wind tunnel for 60 min. The soil movement speed partially depends on the force required to completely separate the topmost soil particles from the lower parts (Chepil, 1956). The wind tunnel flow rate was selected equal to 7 m/s based on the regional wind speed (Fig. 2). First, the collected samples were air-dried around the lake and then the wind tunnel tests were performed for each sample in two modes of spraying of 2% and 7% humidity.

The samples were exposed to air flow at a speed of 7 m/s in the wind tunnel. To show the soil erosion process, the soil samples were scanned using a laser scanner and a three-dimensional profile of the eroded soil was drawn from sampling container surface to examine the erosion process of the samples.

Data analysis

Data were analyzed statistically for significant distribution of data using regression and F-test by SPSS 16 software. Scatter diagrams were drawn in Excel software to find correlation between erosion rates of the samples and the mechanical properties of the soils.

Results and Discussion

Physicochemical properties of soils

There is a complex relationship between soil structure and erodibility because it involves the interaction of many structural factors (Chepil, 1951). A descriptive statistical analysis of the measured features of soils is shown in Table (1). The average percentage of sand particles in this study is higher than those of other particles. The coefficient of variation for clay particles is higher than those of other particles. The changes in the average particle diameter ranges between 0.36 and 3.47 mm.

The soils studied in this region were those with a salinity range of 2.17-8.21 mS/cm. In this region, pH values of saturated extracts in the studied soils ranged from 7.18 to 8.16, with an average of 7.58.

Saline soils contain high concentrations of soluble salts and have EC values > 4 mS. cm^{-1} in the saturated extracts, and sodium soils usually have a high pH (> 8.5) and high (> 15) exchangeable sodium percentage (ESP) (Setia et al., 2011).

The average concentration of soluble calcium (25.8 mEq/l) in the studied samples was higher than those of soluble sodium and magnesium cations (15.18 and 10.27 mEq/l,

respectively). In the study area, SAR varied in the range of 1.3-8.68 $(\mathrm{meq}L^{-1})^{0.5}$. Lack of external drainage and evaporation of solutes increase the salinities of lakes and dried lake beds (Blank et al., 1999). The percentage of moisture was very different (3.96-31.97%) in the dried beds of Lake Bazangan.

Erosion rate

In each experiment, the specific erosion rate was calculated by the grams of sediment lost over the cross-sectional area of the sample container and the experimental duration (Liu et al., 2007). The wind erosion rate of the samples measured in this area varied from 3.21 to 95.63 g/m^2/min at a constant speed of 7 m/s (Table 2). In the studied samples, the soil wind erosion rate was higher for sandy loam texture than for the other textures.

In general, in all samples, increasing humidity from 2 to 7%, due to increased adhesion between soil particles led to a decrease of the rate of soil wind erosion. In the studied samples at the location of sample No. 5 at humidity of 2 and 7%, due to the sandy soil texture of the soil particles, which are light, the rate of soil wind erosion was higher than in the other samples. Sand particles do not tend to retain water in themselves, so there is no adhesion between soil particles in this type of soil texture and they could be quickly moved by creating the wind flow. Also, soil No. 7 with clay texture had the lowest rate of wind erosion. This type of soil texture has a strong tendency to absorb moisture, which increases when the moisture is increased, and the adhesion between the clay particles and aggregates are created with strong bonds. Therefore, when the wind blows, these types of soil particles resist to move.

Table 1- Statistical analysis of the physicochemical features of soils under study

Soil property	Unit	Minimum	Maximum	Mean	Std. Deviation	Coefficient variation
Sand	%	24.4	58.4	39.28	11.18	28.4
Silt	%	26	42	33.11	5.10	15.43
Clay	%	13.6	49.6	27.6	11.26	40.83
d_{50}	mm	0.36	3.47	1.33	1.11	83.6
EC	$\mathrm{mS}.cm^{-1}$	2.17	8.21	3.86	1.91	49.67
pH	-	7.18	8.16	7.58	0.39	5.23
Ca	meq/l	20.36	31.54	25.81	3.17	12.29
Mg	meq/l	0.4	24.03	10.27	9.14	89.05
Na	meq/l	5.04	41.85	15.18	12.89	84.91
SAR	$(\mathrm{meq}L^{-1})^{0.5}$	1.3	8.69	3.41	2.59	76
Moisture Content	%	3.96	31.97	12.66	9.83	77.64
Shear strength	kPa	14.68	26.75	20.4	4.18	20.53

d_{50} Mean particles diameter distribution, EC electrical conductivity, SAR sodium adsorption ratio

Table 2- Measured soil erosion rates (g m−2 min−1) in different 9 sites with wind velocity of 7 m/s at moisture 2% and 7%

Soil erosion rate (g m−2 min−1)									
Region number	1	2	3	4	5	6	7	8	9
Soil texture	Clay Loam	Loam	Loam	Clay Loam	Sandy Loam	Loam	Clay	Clay Loam	Loam
moisture:2%	22.82	74.32	57.03	21.14	95.63	26.25	5.7	16.87	59.5
moisture:7%	6.15	7.64	14.23	16.64	42.29	8.54	3.21	15.97	7.74

 DOI: 10.22055/jise.2021.36299.1948.

Influence of soil physical features

Primary particles of soil

Figure (7) depicts the effect of primary soil particles on the wind-driven soil erosion rate, which generally decreased by increasing clay content (Figure. 7a) due to the fact that clay particles retain more moisture content (Carroll and Oliver, 2005).

By increasing clay content at 2% moisture content, wind erosion rate increased significantly ($R^2 = 0.903$, $p < 0.001$) as an exponential function. At 7% moisture content, the specific erosion rate decreased more significantly ($R^2 = 0.4042$, $p < 0.001$) due to increased moisture and its effect on the formation of clay aggregates with greater strength (Figure. 7a). In general, clay particles can form solid aggregates, which increases the effect of soil texture on water holding capacity by drying the soil. As shown in Figure 6b, there is a positive relationship between sand particle content and the soil erosion rate so that the specific wind erosion rate increases as an exponential function ($R^2 = 0.692$, $p < 0.001$) at 2% moisture as a result of increasing sand particles. Also, the specific wind erosion rate increases ($R^2= 0.6648$, $p < 0.001$) at a moisture content of 7% since sand particles do not tend to retain moisture which is discharged very quickly. Clay particles form a strong bond between the primary soil particles and contribute to the formation of stable aggregates (Ciric et al., 2012).

(Avecilla et al., 2015) found that soils with higher sand particle content had much higher erosion rates than other types. The effect of primary soil particles on wind erosion may be due to the latent effects of other soil properties, including soil mechanical properties (Shahabinejad et al., 2019), which will be discussed below. In the present study, the reduction of clay particles in the samples has led to an increase in soil erosion rate, which is similar to the results of (Korkanc et al., 2008) and (Pérez-Rodríguez et al., 2007).

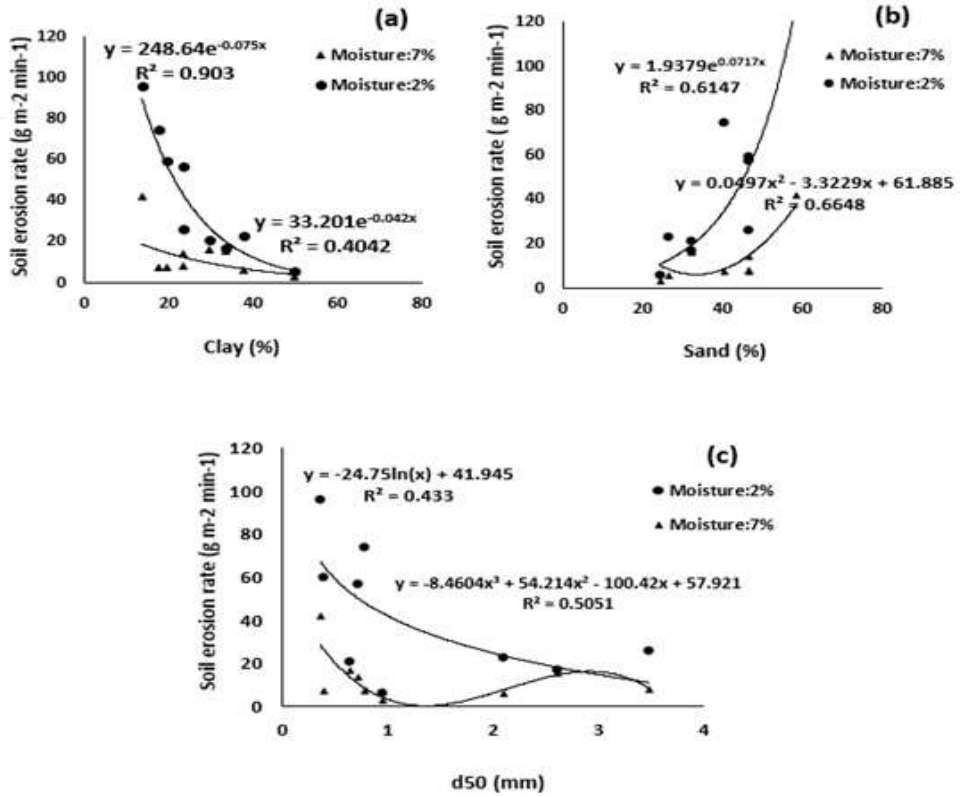

Fig. 7- Influence of different soil particles percentages on soil erosion in the 9 studied regions at two different humidity levels (a) soil moisture 2%, (b) soil moisture (7%) by wind tunnel

Average particle diameter (d50)

Emami et al. (2012) cited a research (Rengasamy and Marchuk, 2011) which showed that the stability of soil aggregates was dependent on the nature of the interaction between water molecules and soil particles. According to Figure 7c, the wind erosion rate decreased as a logarithmic function at 2% ($R^2 = 0.433$, $p < 0.001$) and 7% ($R^2 = 0.5051$, $p < 0.001$) humidity levels by increasing mean particle diameter due to elevated soil surface roughness, which is consistent with the results of (Zamani and Mahmoodabadi, 2013). As shown in the figure, an increase in humidity leads to an increase in the cohesion of soil particles and the wind erosion rate has decreased relative to the content of soil moisture of 2% by increasing soil particle diameter.

Shear strength

The relationship between wind erosion rate and shear strength of the studied soils is shown in Figure (8). According to the Mohr-Coulomb's equation, cohesion and IFA between soil particles influence the soil shear strength. As shown in Figure (8a), there is a negative relationship between particle cohesion and wind erosion rate, which decreases more rapidly as a result of increasing humidity because wind-induced erosion depends on the cohesion force of water around soil particles (Chepil, 1956). By increasing the moisture, the adhesion between soil particles and the resistance of aggregates to separation and transfer is increased and the intensity of wind erosion is decreased. This result is consistent with the findings of (Wiggs et al., 2004) who found that by increasing soil moisture, the intensity of separation and particle transport due to wind erosion is decreased.

Figure (8b) illustrates the relationship between the IFA of soil particles and the wind erosion rate. The IFA depends on the soil texture, particle size distribution, moisture content, particle shape, and dry bulk density. By increasing moisture from 2% to 7%, the amount of internal friction angle and soil wind erosion rate is decreased.

Soil resistance is affected by the exchangeable cations, type, and size of clay particles (Barzegar et al., 1994). Clay and silt particles form bonds between sand particles, which increases soil strength (Emami et al., 2012). Clay particles form tight aggregates between soil particles and control the wind erosion rate.

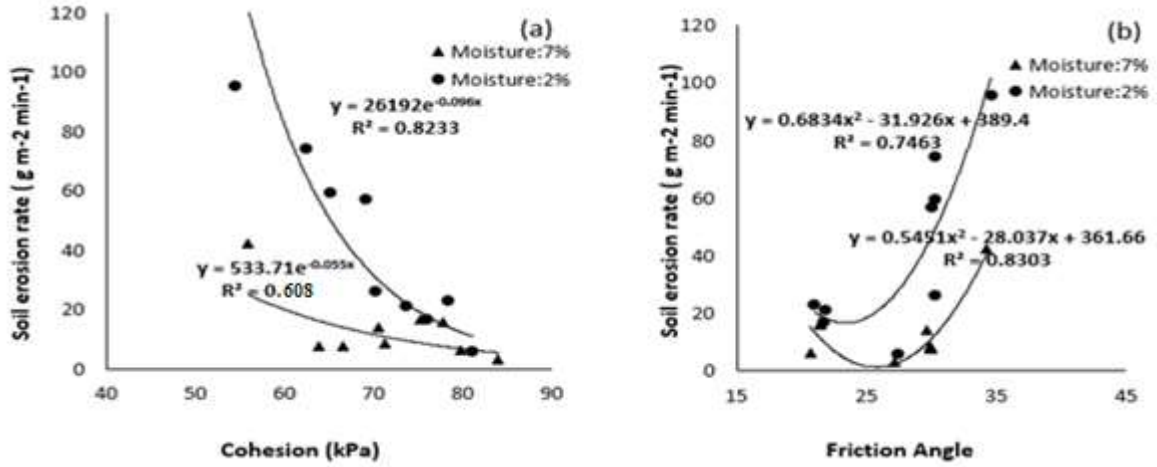

Fig.8- Influence of soil physical properties on soil erodibility erosion at two different humidity levels (a) soil moisture 2%, and (b) soil moisture (7%) by wind tunnel

 DOI: 10.22055/jise.2021.36299.1948.

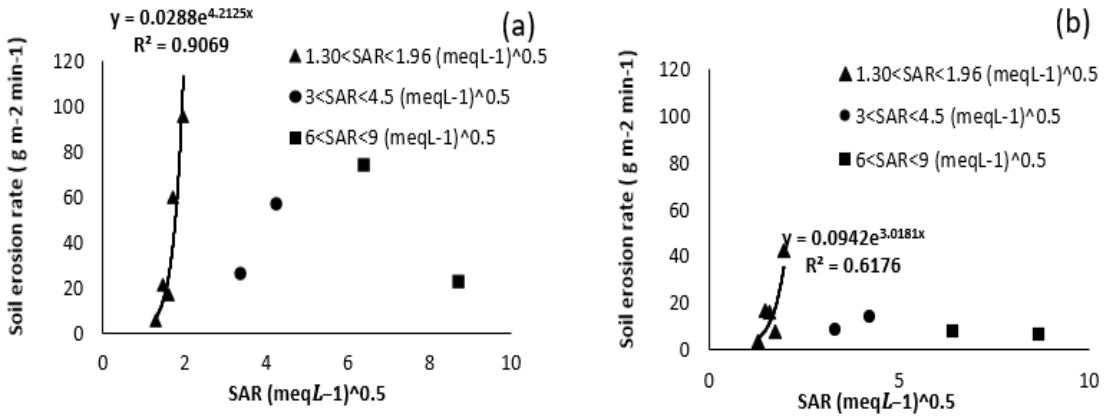

Fig. 9- Influence of Soil salinity on soil erosion at two different humidity levels (a) soil moisture 2%, and (b) soil moisture (7%) by wind tunnel

Table. 3 Cross-validation results of estimating soil erosion rate (Humidity level: 2%)

Parameter	MBE	RMSE	R^2
Clay	-1.6	8.76	0.903
Sand	0.98	19.74	0.614
D50	-0.0003	21.66	0.433
Cohesion	0.99	17.80	0.924
Friction Angle	-0.018	14.49	0.746
SAR	0.14	9.03	0.906

Table. 4 Cross-validation results of estimating soil erosion rate (Humidity level: 7%)

Parameter	MBE	RMES	R^2
Clay	-2.22	9.42	0.404
Sand	-0.03	6.39	0.664
D50	-0.003	7.76	0.505
Cohesion	0.047	6.90	0.608
Friction Angle	-0.02	4.54	0.83
SAR	-1.25	12.75	0.617

Figure (9) shows the relationship between the SAR and the wind erosion rate of soil samples at two different humidity levels. Measurements revealed that at SAR values of 1.30-1.96 (meq$L$−1) ^ 0.5, the erosion rate increased exponentially by increasing soil sodification. An increase in SAR raises the dispersion of clay particles and the crash of aggregates (Barzegar et al., 1994).

Table 3 and Table 4 show the cross-validations result of estimating soil erosion rate at two different humidity levels. The coefficient of determination (R^2), the root mean square error (RMSE), and the mean bias error (MBE) were computed as criteria for the evaluation of the performance of models. These mathematical formulas were calculated as:

$$MBE = \frac{1}{N}\sum_{i=1}^{N}[Z^*(X_i) - Z(X_i)] \quad (6)$$

$$RMSE = \sqrt{\frac{1}{N}\sum_{i=1}^{N}[Z^*(X_i) - Z(X_i)]^2} \quad (7)$$

where z*(xi) and z(xi) are the estimated and observed values at location xi, respectively and N is the number of observations. For an appropriate estimator, MBE should be close to zero, R^2 should be close to 1 and RMSE should be as small as possible.

Fig.10- General view of the Kinect® sensor

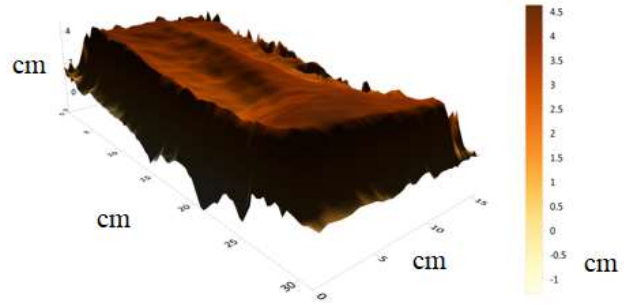

a) Sample 5, Soil moisture:2%

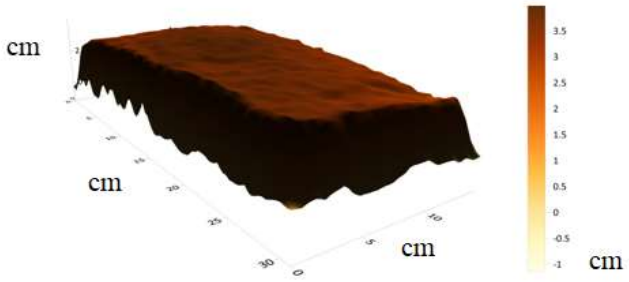

b) Sample 5, Soil moisture:7%

Fig. 11- Three dimensional plots of profiled surface of soil after 60 min

This table indicates that soil physical parameters achieve a slightly smaller RMSE and higher R^2 performs well in predicting soil erosion.

Three-dimensional profile of soil surface erosion

To examine eroded the samples, the surface erosion of soil samples was scanned using a Kinect® sensor (Microsoft). This sensor has three infrared ports, an image depth sensor, and a color camera (RGB) Figure (10). To accurately study soil erosion and soil surface elevation at different distances, images of scanned soil profiles are used to detect changes in erosion rates at different times (Rice et al., 1996). After repeated measurements at a wide range of different surfaces, small standard deviation occurs in the correction of laser scanner sensor used in this experiment and undergoes calibration (Marinello et al., 2015). Then, infrared light was emitted to the soil samples and, after scanning each soil sample, three-dimensional scanned meshes were drawn using the GRAPHER 12 software. Figure (11) shows the profiles of several examples drawn by the Kinect® sensor. Due to having a large number of samples, only a few samples are displayed in this paper.

As can be seen at a moisture content of 2% Figure. (11), the greatest amount of change is observed in the transverse part of the samples in the form of pits and depressions due to the low moisture content. As such, surface soil

particles with less cohesion begin to move and accumulate in the middle part with the onset of soil erosion. As seen in Fig. 10a, because sand particles are the most ingredients making up this sample, and since these light-coarse particles can move easily, the amount of depression and soil loss is higher herein than in the other samples.

Conclusion

In the present study, the potential of specific wind erosion rates was evaluated around Lake Bazangan due to moisture fluctuations in the lake bed. To model wind-induced soil erosion based on the prevailing wind speed in the region, a constant speed of 7 m/s for 60 min was applied to each soil sample at moisture levels of 2% and 7%. Experiments were performed on soil properties to study wind-induced soil erosion. As in previous studies, increasing clay and soil moisture contents significantly reduced wind-induced soil erosion. At 7% moisture, the specific erosion rate decreased as an exponential function ($p < 0.001$, $R = 0.4042$) with a greater intensity than the use of less moisture level due to the effect of moisture on the formation of clay aggregates with high cohesion and increased soil shear strength. Also, the erosion rate increased exponentially by increasing soil sodification due to the effect of SAR on the dispersion of clay particles.

The three-dimensional profile of surface soil erosion, examined by a laser scanner, indicated that sand particles had an important role in increasing the wind-driven soil erosion rate. In general, Figure (11) displays that the erosion rate is much higher in samples with a moisture content of 2%, due to less moisture and cohesion between soil particles, than those with a moisture content of 7%. Finally, the authors appreciate Microsoft Co. and recommend future researchers to employ Microsoft's Kinect® sensor because of easy access and cost-effectiveness for the evaluation of soil movement in critical conditions and, at the same time, examining the standard deviation of generated errors.

Declaration of Competing Interest

There is no conflict to declare.

Acknowledgments

The Research Council of Ferdowsi University of Mashhad is acknowledged for financial support of the project (3/48617). We also thank the anonymous reviewers for their helpful comments.

References

1- Afshar, A.A., Hasanzadeh, Y., Besalatpour, A.A., Pourreza-Bilondi, M., 2017. Climate change forecasting in a mountainous data scarce watershed using CMIP5 models under representative concentration pathways. Theor. Appl. Climatol. 129, 683–699.

2- Anderson, J.D., 2005. Ludwig Prandtl's boundary layer. Phys. Today 58, 42–48.

3- Astm, D., 1994. 3080-90: Standard test method for direct shear test of soils under consolidated drained conditions. Annu. B. ASTM Stand. 4, 290–295.

4- Avecilla, F., Panebianco, J.E., Buschiazzo, D.E., 2015. Variable effects of saltation and soil properties on wind erosion of different textured soils. Aeolian Res. 18, 145–153.

5- Behrouzi-Rad, B., n.d. Difference and Similarity in the Structure of the Population of Water birds Between Natural Bazangan Lake and Shahid Yaghoubi Dam Reservoir. Mar. Sci. 1.

6- Ben-Gal, A., Borochov-Neori, H., Yermiyahu, U., Shani, U., 2009. Is osmotic potential a more appropriate property than electrical conductivity for evaluating whole-plant response to salinity? Environ. Exp. Bot. 65, 232–237.

7- Biglarfadafan, M., Danehkar, A., Pourebrahim, S., Shabani, A.A., Moeinaddini, M., 2016. Application of

Strategic Fuzzy Assessment for Environmental Planning; Case of Bird Watch Zoning in Wetlands. Open J. Geol. https://doi.org/10.4236/ojg.2016.611099

8- Blank, R.R., Young, J.A., Allen, F.L., 1999. Aeolian dust in a saline playa environment, Nevada, USA. J. Arid Environ. 41, 365–381.

9- Carroll, Z.L., Oliver, M.A., 2005. Exploring the spatial relations between soil physical properties and apparent electrical conductivity. Geoderma 128, 354–374.

10- Chen, W., Zhibao, D., Zhenshan, L., Zuotao, Y., 1996. Wind tunnel test of the influence of moisture on the erodibility of loessial sandy loam soils by wind. J. Arid Environ. 34, 391–402.

11- Chepil, W.S., 1956. Influence of moisture on erodibility of soil by wind. Soil Sci. Soc. Am. J. 20, 288–292.

12- Chepil, W.S., 1954. Factors that influence clod structure and erodibility of soil by wind: III. Calcium carbonate and decomposed organic matter. Soil Sci. 77, 473–480.

13- Chepil, W.S., 1951. Properties of soil which influence wind erosion: IV. State of dry aggregate structure. Soil Sci. 72, 387–402.

14- Choobari, O.A., Zawar-Reza, P., Sturman, A., 2014. The global distribution of mineral dust and its impacts on the climate system: A review. Atmos. Res. 138, 152–165.

15- Ciric, V., Manojlovic, M., Nesic, L., Belic, M., 2012. Soil dry aggregate size distribution: effects of soil type and land use. J. soil Sci. plant Nutr. 12, 689–703.

16- Elmore, A.J., Kaste, J.M., Okin, G.S., Fantle, M.S., 2008. Groundwater influences on atmospheric dust generation in deserts. J. Arid Environ. 72, 1753–1765.

17- Emami, H., Astaraei, A.R., Fotovat, A., Khotabaei, M., 2014. Effect of soil conditioners on cation ratio of soil structural stability, structural stability indicators in a sodic soil, and on dry weight of maize. Arid L. Res. Manag. 28, 325–339.

18- Emami, H., Neyshabouri, M.R., Shorafa, M., 2012. Relationships between some soil quality indicators in different agricultural soils from Varamin, Iran.

19- Gile, L.H., Grossman, R.B., 1979. The desert project soil monograph: Soils and landscapes of a desert region astride the Rio Grande Valley near Las Cruces, New Mexico. US Dept. of Agriculture, Soil Conservation Service.

20- Gillette, D., 1978. A wind tunnel simulation of the erosion of soil: Effect of soil texture, sandblasting, wind speed, and soil consolidation on dust production. Atmos. Environ. 12, 1735–1743.

21- Gillies, J.A., Nickling, W.G., Nikolich, G., Etyemezian, V., 2017. A wind tunnel study of the aerodynamic and sand trapping properties of porous mesh 3-dimensional roughness elements. Aeolian Res. 25, 23–35.

22- Gomes, L., Arrue, J.L., Lopez, M. V, Sterk, G., Richard, D., Gracia, R., Sabre, M., Gaudichet, A., Frangi, J.P., 2003. Wind erosion in a semiarid agricultural area of Spain: the WELSONS project. Catena 52, 235–256.

23- Goossens, D., 2004. Effect of soil crusting on the emission and transport of wind-eroded sediment: field measurements on loamy sandy soil. Geomorphology 58, 145–160.

24- Grini, A., Myhre, G., Zender, C.S., Isaksen, I.S.A., 2005. Model simulations of dust sources and transport in the global atmosphere: Effects of soil erodibility and wind speed variability. J. Geophys. Res. Atmos. 110.

25- Ju, T., Li, X., Zhang, H., Cai, X., Song, Y., 2018. Effects of soil moisture on dust emission from 2011 to 2015 observed over the Horqin Sandy Land area, China. Aeolian Res. 32, 14–23.

26- Karimi, A., Khademi, H., Kehl, M., Jalalian, A., 2009. Distribution, lithology and provenance of peridesert loess deposits in northeastern Iran. Geoderma 148, 241–250.

27- Karimi, A., Khormali, F., Wang, X., 2017. Discrimination of sand dunes and loess deposits using grain-size analysis in northeastern Iran. Arab. J. Geosci. 10, 275.

28- Karimi, A., Soodmand, A., Khormali, F., 2014. Grain size parameters of aeolian deposits in Sarakhas area, Norteastern Iran, in: International Symposium on Loess, Soils and Climate Change in Southern Eurasia.

29- Kim, D.S., Cho, G.H., White, B.R., 2000. A wind-tunnel study of atmospheric boundary-layer flow over vegetated surfaces to suppress PM10 emission on Owens (dry) Lake. Boundary-layer Meteorol. 97, 309–329.

30- Korkanc, S.Y., Ozyuvaci, N., Hizal, A., 2008. Impacts of land use conversion on soil properties and soil erodibility. J. Environ. Biol. 29, 363.

31- Liu, D., Abuduwaili, J., Lei, J., Wu, G., Gui, D., 2011. Wind erosion of saline playa sediments and its ecological effects in Ebinur Lake, Xinjiang, China. Environ. Earth Sci. 63, 241–250.

32- Liu, L.-Y., Li, X.-Y., Shi, P.-J., Gao, S.-Y., Wang, J.-H., Ta, W.-Q., Song, Y., Liu, M.-X., Wang, Z., Xiao, B.-L., 2007. Wind erodibility of major soils in the farming-pastoral ecotone of China. J. Arid Environ. 68, 611–623.

33- Maltby, E., Acreman, M.C., 2011. Ecosystem services of wetlands: pathfinder for a new paradigm. Hydrol. Sci. J. 56, 1341–1359.

34- Marinello, F., Pezzuolo, A., Gasparini, F., Arvidsson, J., Sartori, L., 2015. Application of the Kinect sensor for dynamic soil surface characterization. Precis. Agric. 16, 601–612.

35- Munkhtsetseg, E., Shinoda, M., Gillies, J.A., Kimura, R., King, J., Nikolich, G., 2016. Relationships between soil moisture and dust emissions in a bare sandy soil of Mongolia. Particuology 28, 131–137.

36- Nicholson, K.W., 1993. Wind tunnel experiments on the resuspension of particulate material. Atmos. Environ. Part A. Gen. Top. 27, 181–188.

37- Okhravi, R., Amini, A., 2001. Characteristics and provenance of the loess deposits of the Gharatikan watershed in Northeast Iran. Glob. Planet. Change 28, 11–22.

38- Orlovsky, L., Orlovsky, N., Durdyev, A., 2005. Dust storms in Turkmenistan. J. Arid Environ. 60, 83–97.

39- Panayiotopoulos, K.P., Barbayiannis, N., Papatolios, K., 2004. Influence of electrolyte concentration, sodium adsorption ratio, and mechanical disturbance on dispersed clay particle size and critical flocculation concentration in Alfisols. Commun. Soil Sci. Plant Anal. 35, 1415–1434.

40- Pérez-Rodríguez, R., Marques, M.J., Bienes, R., 2007. Spatial variability of the soil erodibility parameters and their relation with the soil map at subgroup level. Sci. Total Environ. 378, 166–173.

41- Pye, K., 1994. Sediment transport and depositional processes.

42- Rengasamy, P., Marchuk, A., 2011. Cation ratio of soil structural stability (CROSS). Soil Res. 49, 280–285.

43- Rice, M.A., Willetts, B.B., McEwan, I.K., 1996. Wind erosion of crusted soil sediments. Earth Surf. Process. Landforms 21, 279–293.

44- Richards, L.A., 1954. Diagnosis and improvement of saline and alkali soils. LWW.

45- Roney, J.A., White, B.R., 2006. Estimating fugitive dust emission rates using an environmental boundary layer wind tunnel. Atmos. Environ. 40, 7668–7685.

46- Shahabinejad, N., Mahmoodabadi, M., Jalalian, A., Chavoshi, E., 2019. In situ field measurement of wind erosion and threshold velocity in relation to soil properties in arid and semiarid environments. Environ. Earth Sci. 78, 501.

47- Shao, Y., 2008. Physics and modelling of wind erosion. Springer Science & Business Media.

48- Singh, H.V., Thompson, A.M., 2016. Effect of antecedent soil moisture content on soil critical shear stress in agricultural watersheds. Geoderma 262, 165–173.

49- Sterk, G., 2003. Causes, consequences and control of wind erosion in Sahelian Africa: a review. L. Degrad. Dev. 14, 95–108.

50- Stetler, L.D., Saxton, K.E., 1997. Analysis of wind data used for predicting soil erosion, in: Proceedings of the Wind Erosion: An International Symposium/Workshop. pp. 3–5.

51- Van Pelt, R.S., Zobeck, T.M., 2007. Chemical constituents of fugitive dust. Environ. Monit. Assess. 130, 3–16.

52- Wiggs, G.F.S., Baird, A.J., Atherton, R.J., 2004. The dynamic effects of moisture on the entrainment and transport of sand by wind. Geomorphology 59, 13–30.

53- Zamani, S., Mahmoodabadi, M., 2013. Effect of particle-size distribution on wind erosion rate and soil erodibility. Arch. Agron. Soil Sci. 59, 1743–1753.

54- Zhang, D.D., Peart, M., Jim, C.Y., He, Y.Q., Li, B.S., Chen, J.A., 2003. Precipitation chemistry of Lhasa and other remote towns, Tibet. Atmos. Environ. 37, 231–240.

55- Zhao, H.-L., Yi, X.-Y., Zhou, R.-L., Zhao, X.-Y., Zhang, T.-H., Drake, S., 2006. Wind erosion and sand accumulation effects on soil properties in Horqin Sandy Farmland, Inner Mongolia. Catena 65, 71–79.

56- Ziyaee, A., Karimi, A., Hirmas, D.R., Kehl, M., Lakzian, A., Khademi, H., Mechem, D.B., 2018. Spatial and temporal variations of airborne dust fallout in Khorasan Razavi Province, Northeastern Iran. Geoderma 326, 42–55.

57- Zobeck, T.M., Baddock, M., Van Pelt, R.S., Tatarko, J., Acosta-Martinez, V., 2013. Soil property effects on wind erosion of organic soils. Aeolian Res. 10, 43–51.